Cellular and Molecular Biology

Dong *et al. Cell. Mol. Biol.*2016, 62 (4): 67-72
ISSN: 1165-158X
doi: 10.14715/cmb/ 2016.62.4.13

Original Research

Molecular and characterization of *NnPPO* cDNA from lotus (*Nelumbo nucifera*) in rhizome browning

C. Dong[1], A. Q. Yu[2], M. G. Yang[1], M. Q. Zhou[3], Z. L. Hu[2*]

[1] College of Biological Engineering, Henan University of Technology, Zhengzhou, Henan 450001, China
[2] State Key Laboratory of Hybrid Rice, College of Life Science, Wuhan University, Wuhan 430072, China
[3] Lotus Center, Wuhan University, Wuhan 430072, China

Abstract: The complete cDNA (*NnPPO*) of polyphenol oxidase in *Nelumbo nucifera* was successfully isolated, using Rapid amplification cDNA end (RACE) assays. The full-length cDNA of *NnPPO* was 2069 bp in size, containing a 1791 bp open reading frame coding 597 amino acids. The putative NnPPO possessed the conserved active sites and domains for PPO function. Phylogenetic analysis revealed that NnPPO shared high homology with PPO of high plants, and the homology modeling proved that NnPPO had the typical structure of PPO family. In order to characterize the role of NnPPO, Real-time PCR assay demonstrated that *NnPPO* mRNA was expressed in different tissues of *N. nucifera* including young leave, rhizome, flower, root and leafstalk, with the highest expression in rhizome. Patterns of *NnPPO* expression in rhizome illustrated its mRNA level was significantly elevated, which was consistent with the change of NnPPO activity during rhizome browning. Therefore, transcriptional activation of *NnPPO* was probably the main reason causing rhizome browning.

Key words: *Nelumbo nucifera*, Polyphenol oxidase, cDNA, Tissue expression, Rhizome browning.

Introduction

Lotus *(Nelumbo nucifera* L.) belongs to Nelumbonaceae, Nymphaeales, which is a perennial aquatic plant. Lotus rhizome is a multipurpose aquatic economic crop in China, with crispy taste and abundant nutrients (1). Mechanical wounding is usually happened during the harvest of lotus rhizome. Rhizome harvested starts browning due to mechanical damage, which leads to the change of product color and flavor, resulting in the loss of nutrients and lost of commercial value. Browning significantly limits the export and domestic sale of lotus rhizome. The process of browning includes two types, that is, enzymatic and nonenzymatic. Nonenzymatic browning is a chemical reaction in foods without the activity of enzymes, knowing as Maillard reaction. Enzymatic reaction catalyzed by polyphenol oxidase (PPO, tyrosinase, E.C. 1.14.18.1) and other enzymes creates melanin and benzoquinone from natural phenols (2), causing millions of dollars losses per year in food industry (3). Phenolic compounds are plant secondary metabolites synthesized mostly through the phenylpropanoid pathway and involve in the defense against invading pathogens (4). PPO widely distributes in fruits and vegetables, having been proved to be the key enzyme causing postharvest pigment degradation, and deterioration for lotus rhizome (5). Recent study illustrated the change of protein profile in lotus rhizome before and after browning (6). Several methods for prevention of PPO activity will be useful in keeping nutrients and commercial value of lotus rhizome, including coating with various package (7) or anti-browning agents for postharvest lotus rhizome (8-11).

Up to date, the isolation and characterization of new *PPO* cDNAs from higher plant are on-going (12, 13). However, as one of important ornamental plant, *NnPPO* cDNA of *N. nucifera* (*NnPPO*) has not been reported. The commercial burden of rhizome causing by PPO gets more attention in the world, it may be of interest to better understand the rationale of isolation and characterization of a new PPO especially from ornamental plant. In the present study, a full-length cDNA sequence of *NnPPO* was cloned and analyzed. The putative sequence of NnPPO was characterized by comparing with other known PPO, performing phylogenetic and 3D structural analysis. Finally, tissue-expression profile of *NnPPO* mRNA including young leave, rhizome, flower, root and leafstalk was detected by Real-time PCR. Additionally, both mRNA and activity of NnPPO were significantly elevated during rhizome browning.

Materials and Methods

Plant material

N. nucifera "Taikonglian-36", which kept in Wuhan University, China was used as material. All the materials were collected and put into liquid nitrogen immediately.

Clone the complete cDNA sequence of *NnPPO* by RACE

The RNA was extracted from young leaves and reverse transcription was performed as the method described (14). According analysis the conservative amino acid sequences, the degenerate primers pair (NnPPO DF and NnPPO DR) was designed to amplify partial NnPPO (Table.1). The settings for the thermal profile included

Received January 8, 2016; **Accepted** April 15, 2016; **Published** April 30, 2016

*** Corresponding author:** Z. L. Hu, State Key Laboratory of Hybrid Rice, Wuhan University, Wuhan 430072, China. Email: huzhongli@whu.edu.cn

Table 1. Names and sequences of primers used in the present study.

Primer name	Sequence (5'-3')
NnPPO DF	TGGCTBTTYTYTTYCCBTTYCAY
NnPPO DR	RWARCTYCCNGCRWAYTC
NnPPO 3GSP1	GCTTGAGAACGTTCCACAT
NnPPO 3GSP2	AACGTCGACCGGATGTGG
NnPPO 5F1	ATGGCGTCNCTNTC
NnPPO 5R1	TTCCAGTAAGGCAACGCAA
NnPPO CF	ATGGCGTCGCTGTCTCCCT
NnPPO CR	TCACGAAGCGAACACTATCTT
NnPPO F	TTCTAATGCCTCCACCTCT
NnPPO R	TTCCTCCTGTCCAACCTC
β-actin F	TGATCGGAATGGAAGC
β-actin R	CAGCAATACCAGGGAAC

an initial denaturing at 94°C for 5 min, followed by 35 cycles of amplification (94°C for 30 s; 55°C for 30 s; and 72°C for 1 min) and a finally extension at 72°C for 10 min. PCR product was inverted into pGEM-T vector (Promega), then product of ligation was transformed into competent *E. coli* DH5α and the fragment was sequenced. Full-length cDNA sequence of *NnPPO* was obtained by the procedures of rapid amplification cDNA ends (RACE) method, using BD SMART™ RACE cDNA Amplification Kit (BD Biosciences Clontech). For the 3'-RACE, the primer sets consisted of NnPPO 3GSP1 with UPM for the first-run PCR, and NnPPO 3GSP2 with NUP for the second-run PCR. Finally, the 5'-RACE was performed using the degenerate prime NnPPO 5F1 and specific primer NnPPO 5R1. The complete cDNA sequence of *NnPPO* was cloned and sequenced, using NnPPO CF and NnPPO CR as primers (Table.1).

Similarity and phylogenetic analysis of NnPPO

Sub-cellular location of NnPPO was evaluated by Protcomp Version 9.0 software. The putative protein sequence of NnPPO was compared with other PPO from NCBI. Multiple sequence alignment was created using CLUSTAL W. And the subsequent phylogenetic tree based on the amino acid sequences was performed by the Parsimony method using the MEGA software version 4 (15).

Homology modeling of NnPPO

The RSCB protein data bank (http://www.rcsb.org/pdb/home/home.do) was used to find the suitable structure templates for homology model. PPO of *Vitis vinifera* (PDB code. 2P3X) was selected as the template (16). The 3D models were constructed by the academic version 6.2 of MODELLER (17) with the default parameters that proposed loop conformations. The qualities of the models were further evaluated by PROCHECK 3.5 (18). The best structural model was chosen, and 3D model of NnPPO was shown by Swiss-pdbviewer 4.1.0 software.

The expression of *NnPPO* mRNA in various tissues

Fresh materials such as young leave, rhizome, flower, root and leafstalk were harvested at reproductive stage. In order to evaluate the expression of *NnPPO* mRNA, *β-actin* (EU131153) was chosen as the reference genes. The special primers for *NnPPO* (NnPPO F and NnPPO R) and *β-actin* (β-actin F and β-actin R) were designed with primers analyzing software Primer Premier 5 (Premier) (Table. 1). Real-time PCR was carried out by DNA binding dye SYBR Green I (TOYOBO) for detection of DNA products. The amplification program consisted of one cycle at 94°C for 30 s, followed by 40 PCR cycles (94°C for 20 s; 60°C for 20 s). According to the method published (14), the primers (NnPPO F and NnPPO R) in Table 1 were designed, and the relative expression of *NnPPO* was calculated using *β-actin* as the reference gene.

***NnPPO* mRNA and activity in rhizome browning**

Lotus rhizome without injury was harvested at reproductive stage. The selected lotus rhizomes were peeled and cut into slices of 0.5 cm thickness and free from nodes after cleaning by running water. The slices were stored at 20°C, and collected at 1 hour post slicing (hps), 2 hps, 3 hps, 4 hps, 6 hps and 8 hps separately, using 0 hps as the control. All the samples were frozen in liquid nitrogen and stored at -20°C for future use. The total RNA was isolated and expression of *NnPPO* mRNA was illustrated by Real-time PCR as method described above. PPO activity of rhizome were assayed based on method (19). In brief, NnPPO enzyme was extracted by homogenizing 20 g rhizome in 40 mL PBS (50 mM, pH=7.0). The supernatant was collected by centrifugation, and NnPPO activity was determined by incubating 0.1 mL enzymatic extract in 1.9 mL PBS (pH=7.0) containing 2.5 mM pyrocatechol at 25°C for 30 min, and absorbance was recorded at 480 nm wavelength. One unit of NnPPO activity was defined as the amount of enzyme that resulted in change of 0.001 absorbance unit per minute. Slices of rhizome were photographed to indicate the scales of browning.

Statistical analysis

Experiments were repeated at least twice to ensure reproducibility. Statistical analysis was performed according to the report (20).

Results

Cloning and sequence analysis of full-length *NnPPO* cDNA

The complete cDNA of *NnPPO* was isolated (FJ999635) by RACE, consisting 2069 bp including the start code ATG, stop code TGA, poly (A) tails, 1794 bp open reading frame, and 275 bp 3′ untranslated regions (Fig. 1). So *NnPPO* cDNA contained the complete

```
1    ATGGCGTCGCTGTCTCCCTTGAATCACACCCTTCTTACTCCCGCTAGCAGTTCTAATGCC
1     M  A  S  L  S  P  L  N  H  T  L  L  T  P  A  S  S  N  A
61   TCCACCTCTCTGTGCCCCTTCAACCAGAGGAGGTCTCAGGTCCCCATAGTCGGCAAGCGT
21    S  T  S  L  C  P  F  N  Q  R  R  S  Q  V  P  I  V  G  K  R
121  CGTTACCGAATGGTTCGTAAGGTCTCATGTGAAGCTACCGATGGAGAAAAGAAACCAACC
41    R  Y  R  M  V  R  K  V  S  C  E  A  T  D  G  E  K  P  T
181  AGATCGGGGAATGAAGAGGGATCTCTCGGGAGGTTGGACAGGAGGAATGTGCTTATTGGT
61    R  S  G  N  E  E  G  S  L  G  R  L  D  R  R  N  V  L  I  G
241  TTAGGAGGCTTGTACGGTGCCACCGGCCTCTGTGCTGGTCGATTGGCATTTGGGGCTCCG
81    L  G  G  L  Y  G  A  T  G  L  C  A  G  R  L  A  F  G  A  P
301  ATCATGCCCCCGGACCTAAGTAAGTGCGGAGCAGCCAACCTGCCCGCCGGCGCAAAGCCC
101   I  M  P  P  D  L  S  K  C  G  A  A  N  L  P  A  G  A  K  P
361  ACCAACCGCTGCCCGCCTGCCAGTTCGGAAATTGTTGACTTCAAGCTGCCATCCTCATCG
121   T  N  R  C  P  P  A  S  S  E  I  V  D  F  K  L  P  S  S  S
421  GAACCCATGCGCGTCAGACCAGCTGCTCACATGGTGGACGAAGAGTATATCGCCAAGTAC
141   E  P  M  R  V  R  P  A  A  H  M  V  D  E  E  Y  I  A  K  Y
481  TCCAAGGCCATTGCCCTCATGAAGGCTCTCCCCGCCGACGACCCACGTAACTTCACGCAA
161   S  K  A  I  A  L  M  K  A  L  P  A  D  D  P  R  N  F  T  Q
541  CAGGCCAATGTTCACTGCGCTTACTGCGATGGAGCTTATGACCAGATTGGTTTCCCGGAC
181   Q  A  N  V  H  C  A  Y  C  D  G  A  Y  D  Q  I  G  F  P  D
601  CTGGAATTACAAGTGCACAACTCGTGGCTGTTTTTCTCATTCCACCGCTACTATCTCTAC
201   L  E  L  Q  V  H  N  S  W  L  F  F  S  F  H  R  Y  Y  L  Y
661  TTCTACGAGAGGATGTTGGGCAAGTTGATCGACGACCCCACATTTGCGTTGCCTTACTGG
221   F  Y  E  R  M  L  G  K  L  I  D  D  P  T  F  A  L  P  Y  W
721  AACTGGGATGCTCCCGCCGGCATGAAAATGCCAACCATGTACGCCAACCCTAACTCCCCT
241   N  W  D  A  P  A  G  M  K  M  P  T  M  Y  A  N  P  N  S  P
781  CTCTACGCAAACTCCGCGATGCCAAGCACCAGCCACCGACGATGATCGATCTCAACTAC
261   L  Y  D  K  L  R  D  A  K  H  Q  P  P  T  M  I  D  L  N  Y
841  AATGTACAAGACACCACGATGACTCCTGAGCAACTACTGAAGAACAATCTCGCCACCATG
281   N  V  Q  D  T  T  M  T  P  E  Q  L  L  K  N  N  L  A  T  M
961  GCCGGAGACCAACCCGACCCTGGTTTCGGGTCGCTTGAGAACGTTCCACATGGACCGGTT
321   A  G  D  Q  P  D  P  G  F  G  S  L  E  N  V  P  H  G  P  V
1021 CATCTATGGGCCGGTGATCGTACCCAGCCTAATATAGAGAATATGGGCAACTTTTACTCG
341   H  L  W  A  G  D  R  T  Q  P  N  I  E  N  M  G  N  F  Y  S
1081 GCTGCCCGAGACCCCATCTTCTATGCCCACCACTCCAACGTCGACCGGATGTGGACAATA
361   A  A  R  D  P  I  F  Y  A  H  H  S  N  V  D  R  M  W  T  I
1141 TGGAAAAAGCTGGGAGGAAGGAGAAAGGATTTCAAAGACCCCGACTGGCTGAACGCGGGC
381   W  K  K  L  G  G  R  R  K  D  F  K  D  P  D  W  L  N  A  G
1201 TTCCTGTTGTACGACGAGAACAAGCAGCTGGTGAGAGTTAAGGTTCGGGACTGCCTGGAC
401   F  L  L  Y  D  E  N  K  Q  L  V  R  V  K  V  R  D  C  L  D
1261 GAGAAGAAACTCCGGTACTCGTATCAGGACGTGGAGATTCCATGGATGAAGACGAGGCCC
421   E  K  K  L  R  Y  S  Y  Q  D  V  E  I  P  W  M  K  T  R  P
1321 ACGCCTGGTAAACTCATGGCAGCTGCTCAGAAACTGAAGATTACGGATAGGGGGTTGAAG
441   T  P  G  K  L  M  A  A  Q  K  L  K  I  T  D  R  G  L  K
1381 AAGAAGAAGCCAACCGTCAGTGAGTTCCCCAAAGAACTTGATGCGCCATTCAAGGTAGTG
461   K  K  K  P  T  V  S  E  F  P  K  E  L  D  A  P  F  K  V  V
1441 GTGAAGAGGCCGAGGAAATCGAGGAGCAAGAAAGAGAAGGAGCGAAGAGGAGATATTG
481   V  K  R  P  R  K  S  R  S  K  K  E  K  E  D  E  E  E  I  L
1501 GTAATAGACCAAGTAGAGTTGGAGAGGGACACGGTGGTGAAGTTCGACGTCTACATCAAC
501   V  I  D  Q  V  E  L  E  R  D  T  V  V  K  F  D  V  Y  I  N
1561 GACGAGGACGAGCCAAGCCCGGATAAGAGTGAGTTCGCCGGGAGCTTTGTGAATGTTCCC
521   D  E  D  E  P  S  P  D  K  S  E  F  A  G  S  F  V  N  V  P
1621 CACAAGCACGGGAAGAAGATGAGCAAGCTTAAGACGTGCCTGAGATTCGGTATCTCGGAA
541   H  K  H  G  K  K  M  S  K  L  K  T  C  L  R  F  G  I  S  E
1681 TTGCTGGAGGACTTGGAAGCCGAAGATGACGACGAGGTGGTGGTGACTATAGTACCAAGG
561   L  L  E  D  L  E  A  E  D  D  D  E  V  V  V  T  I  V  P  R
1741 ATCGGAGGGGACCTTGTCACCATTGGTGGGATCAAGATAGTGTTCGCTTCGTGATTTGTT
581   I  G  G  D  L  V  T  I  G  G  I  K  I  V  F  A  S  *
1801 ACTGCGTGTAGGAATCCTCCTTTTGTTTGTTTCAATTTATTGTATTTTCCCCCTTTGCCT
1861 TTTTGAATAAGTTTGAAGCAGCATCCACCCCAGTTCCAGTTTAGGTTTTTGGTGGATCAC
1921 GACGTGGAGTACTCCTAAGATGTGTAACCGGAGAAAGAACTACCGGAGGTGGTTGCCTCT
1981 GTAGTCAACGACTCCAATGCTTAATATTTTGTTGAAGGATAAACAGGAGAAAATTTTCT
2041 GAAAAAAAAAAAAAAAAAAAAAAAAAAAAA
```

Figure 1. Nucleotide and deduced amino acid sequence of NnPPO. The cDNA sequence of *NnPPO* had been deposited in GenBank (FJ999635). The asterisk (*) indicated the stop codon. Both CuA ([185]HCAYCDGAYDQIGFPDLELQVHNSWLFFS-FHRYYLYFYERMLGKLID DPTFALPYWNWD[243]) and CuB ([337]HGPVHLWAGDRTQPNIENMGNFYSAARDPIFYA HHSNVDRMWTIW[381]) domains were underlined. Several His coordinating a copper ion and comprising the active sites, including H^{185}, H^{206}, H^{215} for CuA and H^{337}, H^{341}, H^{371} for CuB were boxed. The C-terminal end of NnPPO consisting of conserved PPO1_DWL and PPO1_KFDV domains were circled.

opening reading frame and 3'UTR, and it could not be concluded if there were 5' UTR upstream

of the ATG. The putative NnPPO contained 597 amino acids, and the molecular weight of NnPPO was about 56.8 KD with isoelectric point 8.6. NnPPO belonged to tyrosinase superfamily. Protcomp Version 9.0 software indicated NnPPO protein sub-cellular located in chloroplast. NnPPO was a copper-binding metalloprotein, consisting two conserved copper-binding domains (CuA and CuB) and a C-terminal extension. CuA and CuB domains were 59 and 45 amino acids in length respectively, separately by a linker segment of 93 residues. Both CuA ([185]HCAYCDGAYDQIGFPDLELQVHNSW LFFS-FHRYY LYFYERMLGKLIDDPTFALPYWNWD[243]) and CuB ([337]HGPVHLWAGDRTQPNIENM GNFY-SAARDPIFYAHHSNVDRMWTIW[381]) had three His that coordinated a copper ion and comprised the active sites, including H^{185}, H^{206}, H^{215} for CuA and H^{337}, H^{341}, H^{371} for CuB. The C-terminal end of NnPPO consisted of a PPO1_DWL and a PPO1_KFDV domain (Fig. 1).

Similarity and phylogenetic analysis of NnPPO

The multiple alignment of NnPPO was performed by selecting PPO sequences of ten representative species from high plants including *Camellia nitidissima* (ACM43505.1), *Vitis labrusca x Vitis vinifera* (BAO79387.1), *Dimocarpus longan* (AKJ70977.1), *Eriobotrya japonica* (AFO55217.1), *Gossypium hirsutum* (AII22006.1), *Pyrus pyrifolia* (BAB64530.1), *Morus alba var. multicaulis* (ALF12287.1), *Litchi chinensis* (AEQ30073.1), *Morus notabilis* (EXB82817.1) and *Pyrus x bretschneideri* (ABS88291.1). Additionally, the copper-binding domains, PPO1_DWL and PPO1_KFDV were aligned with respective motifs from the selected species (Fig. 2). The deduced amino acid sequences of NnPPO showed similarities with high plant (40 % -60 %). The phylogenetic analysis indicated NnPPO grouped together with high plants and provided evidence that PPO in different species had been derived from a common ancestor (Fig. 3).

The homology model of NnPPO

In order to understand structure-function relationship, the putative three-dimensional structure of NnPPO was constructed by homology modeled using the known structures of *Vitis vinifera* PPO (PDB code. 2P3X). The NnPPO and template protein shared a high degree of ho-

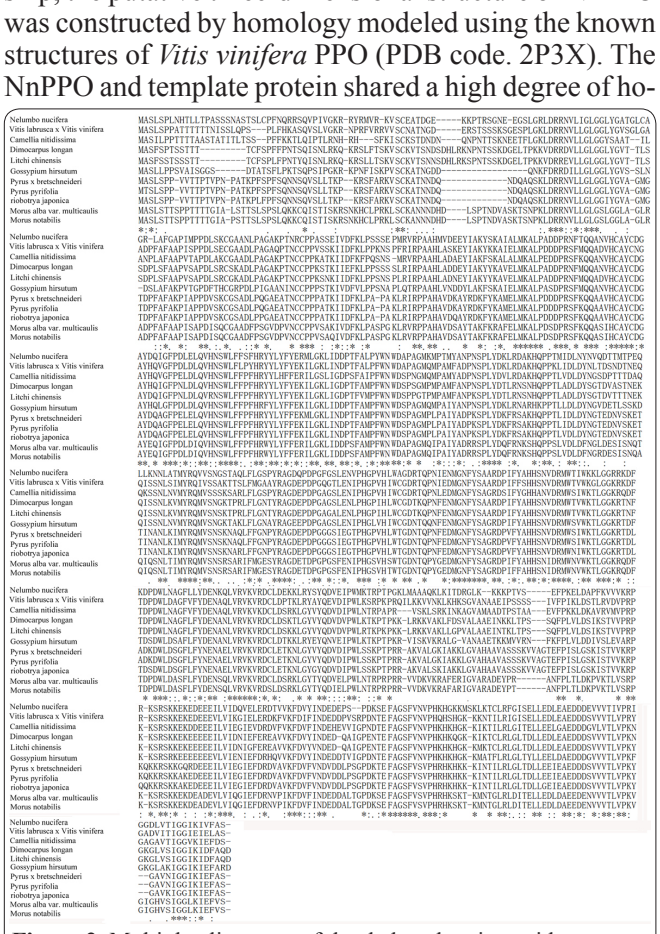

Figure 2. Multiple alignment of the deduced amino acid sequence of NnPPO in present study with PPO proteins from high plants. The conserved CuA and CuB domains were boxed, and C-terminal motifs of DWL and KFDV were underlined. GeneBank accession numbers for the compared sequences were the same as the numbers used in Figure 3.

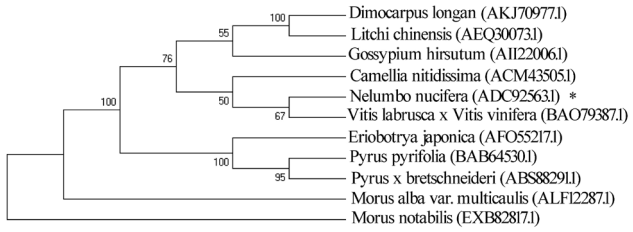

Figure 3. Phylogenetic analysis of NnPPO was performed by neighbour-joining method using MEGA4 software. Numbers in the branches represented the bootstrap values (%) from 100 replicates.

mology (65 %), suggesting a high reliability of predicted structure. The 3D structure of NnPPO was generated by MODELLER software. The Ramachandran plot (data not shown) provided by PROCHECK demonstrated that most of model residues were in most favorable regions, and none of residues in generously allowed regions and disallowed regions. The two conserved copper-binding domains (CuA and CuB) and C-terminal extension (PPO1_DWL and PPO1_KFDV domain) were shown by Swiss-pdbviewer 4.1.0 (Fig. 4).

Data analysis of Real-time PCR and enzymatic activity

For the aim of investigating the expression profile of *NnPPO*, Real-time PCR was performed using *β-actin* as reference gene. The $2^{-\Delta\Delta Ct}$ methods could be used to calculate the relative quantity. *NnPPO* mRNA was detected in various tissues of *N. nucifera* including young leave, rhizome, flower, root and leafstalk at reproductive stage. The relative expression of *NnPPO* mRNA was calculated by comparing with flower. As shown in the figure 5a, the highest expression of *NnPPO* mRNA was found in rhizome (4 fold). mRNA level of leave (2.7 fold) and leafstalk (2.5 fold) was at moderate level, while it was still more than root (1.6 fold). Additionally, Real-time PCR analysis indicated browning elevated the expression of *NnPPO* mRNA in rhizome, using 0 hps as the control. It seemed that *NnPPO* mRNA started to increase at 1 hps, while the difference was not significant ($p<0.05$). The level of *NnPPO* mRNA was significantly elevated as soon as 2 hps (1.6 fold), showing little change at 3 hps (1.6 fold). It continued to increase at 4 hps (1.9 fold), and then the level was relatively stable at 6 hps (2.0 fold) and 8 hps (2.1 fold) (Fig. 5b). The NnPPO activity was about 27 U/mg in intact rhizome (Fig. 5c), increasing to 49 U/mg at 1 hps, 44 U/mg at 2 hps and 41 U/mg at 3 hps. Then the NnPPO activity reached the higher level at 4 hps (96 U/mg), 6 hps (98 U/mg) and 8 hps (88 U/mg). Additionally, there was no browning in slice of rhizome at 0 hps. As the browning time increasing, the areas of browning spots were augmented (Fig. 5d).

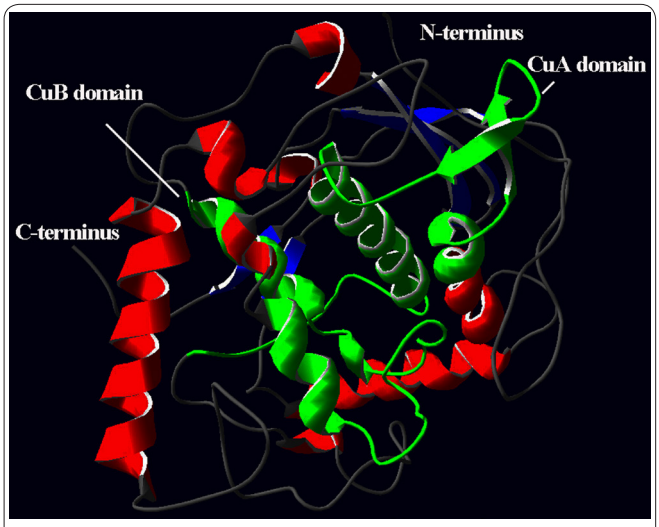

Figure 4. The predicted 3D structure of NnPPO. The N-terminus and C-terminus were shown. α-helix, β-sheet and coils were labeled by red, blue and white colors respectively. The CuA and CuB domains were represented by green color.

Discussion

The full-length cDNA sequence of *NnPPO* was cloned and characterized, possessing all the main characteristic amino acid residues, and motifs of PPO protein family. Sequence and multiple alignment showed that CuA and CuB domains were conserved in NnPPO. The first residues of CuA domain occurred at the beginning of a HXXXC motif (21), commonly known as HCAYC. The second Cys^{189} of HCAYC motif was predicted to form a thioether bond with the second conserved His^{206} of the CuA domain. In the CuB domain, the first two conserved His residues (H^{337} and H^{341}) were included in a previously unidentified HxxxH sequence motif (Fig.

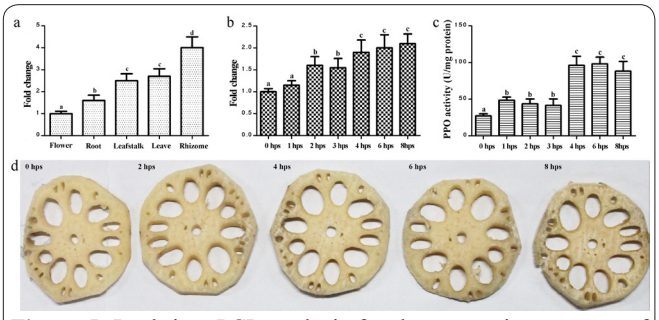

Figure 5. Real-time PCR analysis for the expression patterns of *NnPPO* mRNA in various tissues and during rhizome browning. a. Relative amounts of *NnPPO* mRNA in various tissues. Total RNA was isolated from young leave, rhizome, flower, root and leafstalk, and mRNA level of *NnPPO* was examined by Real-time PCR using *β-actin* as the reference gene. The highest expression of *NnPPO* mRNA was found in rhizome. mRNA level of leave and leafstalk was at moderate level, while it was still more than root, and the lowest expression of *NnPPO* was detected in flower. b. The expression of *NnPPO* mRNA was detected in response to rhizome browning. The fresh-cut lotus slices and intact rhizome were stored at 20°C, and collected at 1 hour post slicing (hps), 2 hps, 3 hps, 4 hps, 6 hps and 8 hps separately, using intact rhizome as control. Real-time PCR analysis indicated that *NnPPO* mRNA up-regulated at 1 hps, while the difference was not significant ($p<0.05$). *NnPPO* mRNA was significantly elevated as soon as 2 hps (1.6 fold), showing little change at 3 hps (1.6 fold). *NnPPO* mRNA continued to increase at 4 hps (1.9 fold), and then the level was relatively stable at 6 hps (2.0 fold) and 8 hps (2.1 fold). c. The NnPPO activity was about 27 U/mg in intact rhizome (Fig. 5c), increasing to 49 U/mg at 1 hps, 44 U/mg at 2 hps and 41 U/mg at 3 hps. Then the NnPPO activity reached the higher level at 4 hps (96 U/mg), 6 hps (98 U/mg) and 8 hps (88 U/mg). Different letters represented significant difference at $p<0.05$. d. The photographs of browning rhizome at 0 hps, 2 hps, 4 hps, 6 hps and 8 hps.

1 and 2). NnPPO protein sub-cellular located in chloroplast. Experimental proof of a non-plastidic location for PPO proteins had only been achieved for PtrPPO13 from poplar and AmAS1 from snapdragon (22, 23). The phylogenetic analysis indicated NnPPO grouped together with plant PPO and provided evidence that all PPOs had been derived from a common ancestor (Fig. 3). NnPPO showed high homology (65 %) with *Vitis vinifera* PPO. The structural model comparison results showed that copper binding domains and C-terminal extension of NnPPO were conserved and matched with *Vitis vinifera* PPO, suggesting their functional similarity. The homology model illustrated CuA consisted two α-helix and β-sheet, while CuB contained three α-helix (Fig. 4).

PPO was widely known to be involved in enzymatic browning reaction in many fruits and vegetables including lotus rhizome with various catalytic mechanisms. Many studies had focused on PPO expression in relation to tissue browning and food processing (12, 13). According to previous browning model, tissue browning of plant resulted from the phenols oxidation into quinones by PPO in the presence of oxygen. In this study, we have cloned and characterized the expression of a browning-induced *NnPPO*. Tissue expression of *NnPPO* mRNA was investigated by Real-time PCR in root, flower, young leave, leafstalk as well as rhizome. *NnPPO* mRNAs were detected in various tissue types, showing a broad pattern of expression. The levels of *NnPPO* mRNAs in rhizome (4 fold), young leave (2.7 fold), leafstalk (2.5 fold) and root (1.6 fold) were relative higher than the expression of *NnPPO* in flower (Fig. 5a). The expression profile illustrated *NnPPO* was uniformly distributed in different tissues, which was consistent with the result that *PPO* played various roles in different development stages or tissues (23). Additionally, it seemed that the *NnPPO* produced in rhizome known as the meristem of *N. nucifera* was probably transported to other tissues in developmental stage. It was speculated that postharvest wounding in lotus rhizome irreversibly resulted in the up-regulation of NnPPO mRNA and activity, triggering rhizome browning occurrence (Fig. 5b and 5c). Additionally, combination the NnPPO results of mRNA and activity during rhizome browning illustrated systemic induction of NnPPO activity was due to an increasing abundance of *NnPPO* transcript accumulation. Therefore, transcriptional activation of *NnPPO* was probably the main reason causing rhizome browning (Fig. 5d). In future experiment, we will currently try to develop transgenic plants in order to understand the mechanism of NnPPO in aquatic plant.

Acknowledgments

The authors are greatly appreciative of the reviewers for their helpful comments and detailed suggestions. This work is financially supported by the National Science and Technology Supporting Program (no. 2012BAD27B01), Foundation of Henan Educational Committee (no. 16A180024; no. 12A180006), Doctoral Scientific Research Start-up Foundation from Henan University of Technology (no. 31400855), and Fundamental Research Funds for the Henan Provincial Colleges and Universities in Henan University of Technology (no. 2015QNJH07).

References

1. Xing Y, Li X, Xu Q, Jiang Y, Yun J, Li W. Effects of chitosan-based coating and modified atmosphere packaging (MAP) on browning and shelf life of fresh-cut lotus root (Nelumbo nucifera Gerth). Innov Food Sci Emerg 2010; 11: 684 –689.

2. Xu YQ, Yin JF, Yuan HB, Chen JX, Wang F. Research advances of browning during processing of fruits and vegetables (in Chinese). Storage Process 2007; 7 (3): 11 − 14.

3. Grotheer P, Valles S, Simonne A, Kim JM, Marshall MR. Polyphenol oxidase inhibitor(s) from german cockroach (blattella germanica) extract. J Food Biochem 2012; 36: 292-300.

4. Pati S, Losito I, Palmisano F, Zambonin P. Characterization of caffeic acid enzymatic oxidation by-products by liquid chromography coupled to electrospray ionization tandem mass spectrometry. J Chrom A 2006; 1102: 184–92.

5. Li J, Wang QZ. Enzyme browning in lotus rhizome and its inhibition. Shanxi Food Ind 2000; 2: 10–12.

6. Jiang J, Jiang L, Zhang L, Luo H, Opiyo AM, Yu Z. Changes of protein profile in fresh -cut lotus tuber before and after browning. J Agric Food Chem 2012; 60(15): 3955-65.

7. Wang QZ, Li J. Effect of package materials on keeping quality of lotus rhizome. Stored Process 2002; 2(2): 9–11.

8. Luo JG, Li J, Wang QZ. Study on the browning inhibition in fresh cut of lotus rhizome. Food Res Dev 2006; 27(6): 74–76.

9. Duan XW, Su XG, You YL, Qu HX, Li YB, Jiang YM. Effect of nitricoxide on pericarp browning of harvested longan fruit in relation to phenolic metabolism. Food Chem 2007; 104: 571–576.

10. Chitbanchong W, Sardsud W, Whangchai K, Koslanund R, Thobunluepop P. Minimally of polyphenol oxidase activity and controlling of rotting and browning of longan fruits cv. DAW by SO2 treatment under cold storage conditions. Int J Agric Res 2009; 4: 349–361.

11. Apai W. Effects of fruit dipping in hydrochloric acid then rinsing in water on fruit decay and browning of longan fruit. Crop Prot 2010; 29: 1184–1189.

12. Constabel CP, Yip L, Patton JJ, Christopher ME. Polyphenol oxidase from hybrid poplar. Cloning and expression in response to wounding and herbivory. Plant Physiol 2000; 124(1): 285-95.

13. Sanchez-Amat A, Patricia Lucas E, Eva F, Jose Carlos Garcia B, Francisco S. Molecular cloning and functional characterization of a unique multipotent polyphenol oxidase from Marinomonas mediterranea. Biochim Biophys Acta 2001; 1547(1): 104-16.

14. Dong C, Zheng XF, Li GL, Zhu HL, Zhou MQ, Hu ZL. Molecular cloning and expression of two cytosolic copper-zinc superoxide dismutases genes from Nelumbo nucifera. Appl Biochem Biotechnol 2011; 163 (5): 679-691.

15. Tamura K, Dudley J, Nei M, Kumar S. MEGA4: Molecular Evolutionary Genetics Analysis (MEGA) software version 4.0. Mol Biol Evol 2007; 24: 1596-1599.

16. Reyes Grajeda JP, Virador VM, Blanco-Labra A, Mendiola-Olaya E, Smith GM, Moreno A, Whitaker JR. Cloning, sequencing, purification, and crystal structure of Grenache (Vitis vinifera) polyphenol oxidase. J Agric Food Chem 2010; 58: 1189-1201.

17. Sanchez R, Sali A. Evaluation of comparative protein structure modeling by MODELLER -3. Proteins (Suppl) 1997; 1: 50-58.

18. Laskowski RA, MacArthur MW, Moss DS, Thornton JM. Procheck: a program to check the stereochemical quality of protein structures. J Appl Crystallogr 1993; 26: 283-291.

19. Zhan L, Hu J, Lim L, Pang L, Li Y, Shao J. Light exposure inhibiting tissue browning and improving antioxidant capacity of fresh-cut celery (Apium graveolens var. dulce). Food Chem 2013; 141:

2473 –2478.
20. Babic M, Radic S, Cvjetko P, Roje V, Pevalek-Kozlina B, Pavlica M. Antioxidative response of Lemna minor plants exposed to thallium(I)-acetate. Aquat Bot 2009; 91: 166-172.
21. Tran LT, John ST. Constabel CP. The polyphenol oxidase gene family in land plants: Lineage-specific duplication and expansion. BMC Genomic 2012; 13: 395.
22. Tran LT, Constabel CP. The polyphenol oxidase gene family in poplar: phylogeny, differential expression and identification of a novel, vacuolar isoform. Planta 2011; 234: 799– 813.
23. Ono E, Hatayama M, Isono Y, Sato T, Watanabe R, Yonekura-Sakakibara K, Fukuchi-Mizutani M, Tanaka Y, Kusumi T, Nishino T, Nakayama T. Localization of a flavonoid biosynthetic polyphenol oxidase in vacuoles. Plant J 2006; 45: 133– 143.